

11A.3 A MULTI-DOPPLER RADAR ANALYSIS OF INTERSECTING BOUNDARIES DURING THE INTERNATIONAL H₂O PROJECT (IHOP)

CHRISTINA D. HANNON* AND PAUL MARKOWSKI

Department of Meteorology, Pennsylvania State University, University Park, PA

1. INTRODUCTION

The International H₂O Project (IHOP) consisted of a large array of instrumentation including, but not limited to, aircraft, mobile radars (ground-based and airborne), mobile soundings, dropsondes, mobile mesonets, lidar, radiometers, and special NWS rawinsonde launches. One of the goals of IHOP was to investigate the distribution of water vapor leading to convection initiation (CI). There have been many observational and modeling studies of convection associated with the dryline or other boundaries to understand CI, but data with the spatial and temporal resolution of those collected during IHOP have not previously been obtained. This paper presents data collected from the 12 June 2002 CI mission and seeks to understand why convection failed to be initiated despite the formation of deep cumulus clouds within the intensive observing region (IOR).

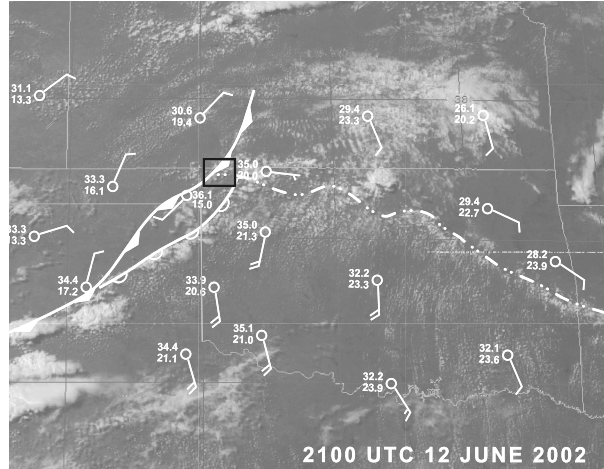


FIG. 1. Visible satellite imagery at 2100 UTC 12 June 2002, using conventional symbology to depict boundary locations. Station models show winds barbs in knots, and temperature and dewpoint in °C. The black rectangular region represents the radar domain depicted in Fig. 2

2. MESOSCALE ENVIRONMENT

The Shared Mobile Atmospheric Research and Teaching Radar (SMART-R), the University of Connecticut XPOL mobile radar, and two Doppler-On-Wheels radars (DOW2, DOW3) were deployed on 12 June 2002 in the Oklahoma panhandle to observe several mesoscale boundaries including a nearly stationary outflow boundary, a cold front, and a dryline (Fig. 1). Data were collected continuously from approximately 1930–2145 UTC from all four radars during the third deployment (Fig. 2).

An old outflow boundary from overnight convection was oriented west-east and remained nearly stationary (moving $< 2 \text{ m s}^{-1}$) during data collection. The outflow boundary intersected a north-south oriented dryline to the east of the radar domain and a cold front within the domain. A mesoscale circulation was reported in surface observations near the vicinity of Slapout, OK around 1945 UTC (not shown). Numerous dust devils were reported and several were large and long-lived. Convection was initiated 40 km east of the center of IOR, in western Woods County, OK at 2050 UTC and rapidly intensified.

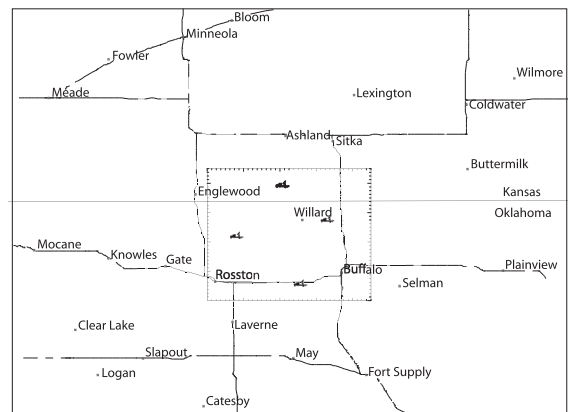


FIG. 2. Map of the area in which the radar data were analyzed. The box represents the $36 \times 36 \text{ km}$. The location of the radars within the domain are shown, as well as major state highways and surrounding towns.

*Corresponding author address: Christina D. Hannon, Department of Meteorology, Pennsylvania State University, 503 Walker Building, University Park, PA 16802; e-mail: cdh181@psu.edu.

3. DATA AND METHODOLOGY

The radar data were edited to remove erroneous velocities due to noise, ground clutter, second trip echos, and aliasing. The radial velocity data were interpolated to a Cartesian grid using a Barnes objective analysis (Barnes 1964). The weighting function, κ was chosen to be 0.04 km^2 . Grid spacings of 100 m in the horizontal and vertical were used. The grid spans $36 \times 36 \text{ km}$ in the horizontal and 2 km in the vertical, and is centered at $36^\circ 56' \text{ N}$, $99^\circ 45' \text{ W}$, approximately at the center of the IOR.

Three-dimensional wind syntheses were produced using the overdetermined dual-Doppler approach and the anelastic mass continuity equation integrated upward. From the horizontal wind field, vertical velocity, horizontal divergence, and vertical vorticity fields were computed. Data were interpolated every 90 seconds from three radars, with four radars contributing every 180 seconds. *Analyses herein only consider grid points at which at least three of the four radars contributed.*

4. RESULTS

There are several interesting observations during the third deployment. The first observation is the complexity of the boundary layer (Figs. 3–8). There are many circulations present in the horizontal and vertical cross sections that the current observational network cannot resolve. Resolving these circulations is not surprising due to the high temporal and spatial resolution of the dataset, but the complexity within the domain is surprising. Due to the complexity of the three-dimensional wind field and without the thermodynamic information, the placement of the cold front is questionable. Regardless, it is seen that the front is not a smooth boundary as presented in conceptual models. Updrafts along the front are of the same magnitude or less than those associated with boundary layer convective cells. Horizontal convective rolls are present as well as less organized boundary layer convection. The maximum vertical velocities exceed 3 m s^{-1} at an altitude of 500 m, and increase to over 6 m s^{-1} at higher altitudes.

The second observation is the vertical continuity of vertical vorticity. The maxima of vertical vorticity seen in Figs. 5 and 8 represent columns of vertical vorticity. The columns extend 1 km and are nearly upright in the vertical, even in the stronger flow. As well as vertical coherency, the vertical vorticity columns have temporal continuity. The oral presentation will show the vorticity maxima were advected by the flow using animations. The maximum values of vertical vorticity were $O(10^2 \text{ s}^{-1})$.

The third observation that was found to be interesting was the low correlation between vertical velocity and vertical vorticity. The correlation, at all analysis times and all levels within the domain, was less than 0.33. The correlations were computed over the entire domain, near and away from the mesoscale boundaries. It may be possible that correlations would be greater when considering smaller areas consisting of only the mesoscale boundaries. In a study of the convective boundary layer using

a large-eddy simulation, Kanak et al. (2000) found local maxima in vertical velocity were collocated with vertical vorticity. The simulations did not consider the presence of any mesoscale boundaries. In the wind syntheses near the cold front, the collocation of maxima in vertical velocity and vertical vorticity are frequent. Several IHOP investigators hypothesize that the existence of such features near mesoscale boundaries may lead to CI. It will be interesting to study the thermodynamic fields near the mesoscale boundaries to determine the failure of CI within the domain.

5. FUTURE WORK

There are several goals to accomplish in determining the failure of CI for this domain. The most challenging will be to ascertain the four-dimensional virtual potential temperature and moisture fields, which will be combined with the wind analyses. Positions of clouds within the analysis domain will be documented to compare with maxima in vertical velocity, vertical vorticity, virtual potential temperature, and water vapor mixing ratios. Furthermore, air parcel trajectories into the clouds will be computed. This analysis is hoped to be combined with those already completed to assess changes in the given fields along the parcel path. The ultimate goal is to better understand why convection failed to be initiated within the domain using all of the data available.

Acknowledgments. We are thankful for comments provided by Conrad Ziegler, Erik Rasmussen, Yvette Richardson, and Josh Wurman. We are also grateful to Curtis Alexander, Nettie Arnott, and Mike Buban, who provided support in obtaining and editing radar data, and all those who gave their time to participate in IHOP. Radar editing was performed using the NCAR SOLO software. The NCAR REORDER software was used to perform the objective analysis of radial velocity data. Wind synthesis were performed using the NCAR CEDRIC software.

REFERENCES

- Barnes, S. L., 1964: A technique for maximizing details in numerical weather maps analysis. *J. Appl. Meteor.*, **3**, 396-409.
- Kanak, K. M., D. K. Lilly, and J. T. Snow, 2000: The formation of vertical vortices in the convective boundary layer. *Quart. J. Royal Meteor. Soc.*, **126**, 2789-2810.
- Oye, R., and M. Case, 1992: REORDER- A program for gridding radar data: Installation and use manual for the UNIX version. NCAR, 22pp. [Available from Field Observing Facility, National Center for Atmospheric Research, P.O. Box 3000, Boulder, CO, 80307.]
- , C. K. Mueller, and S. Smith, 1995: Software for radar translation, visualizations, editing, and interpolation. Preprints, *27th Conf. On Radar Meteorology*, Vail, CO, Amer. Meteor. Soc., 359-361.

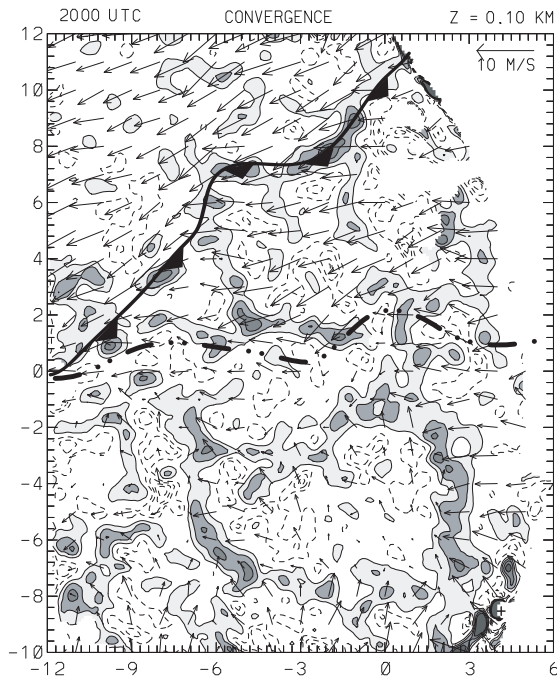


FIG. 3. Horizontal convergence, $-\nabla \cdot \mathbf{v}_h$, for 2000 UTC 12 June 2002 at an altitude of 100 m. Positive (negative) contours are solid (dashed) and contoured every $2.5 \times 10^{-3} \text{ s}^{-1}$ beginning at $1.5 \times 10^{-3} \text{ s}^{-1}$ ($-1.5 \times 10^{-3} \text{ s}^{-1}$). Areas exceeding $1.5 \times 10^{-3} \text{ s}^{-1}$ are shaded. Horizontal wind vectors are overlaid for every 10th grid point. The axes have units of km. The cold front is indicated using conventional symbology and and outflow boundary is indicated using the dash dotted line

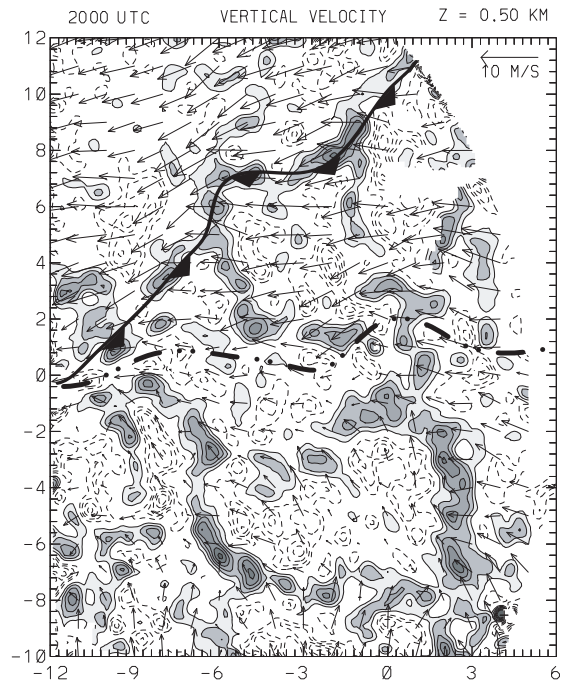


FIG. 4. Vertical velocity, w , for 2000 UTC 12 June 2002 at an altitude of 500 m. Positive (negative) contours are solid (dashed) and contoured every $0.5 \times 10^{-3} \text{ s}^{-1}$ beginning at $0.5 \times 10^{-3} \text{ s}^{-1}$ ($-0.5 \times 10^{-3} \text{ s}^{-1}$). Areas exceeding $0.5 \times 10^{-3} \text{ s}^{-1}$ are shaded. Horizontal wind vectors are overlaid for every 10th grid point. The axes have units of km. The cold front is indicated using conventional symbology and and outflow boundary is indicated using the dash dotted line

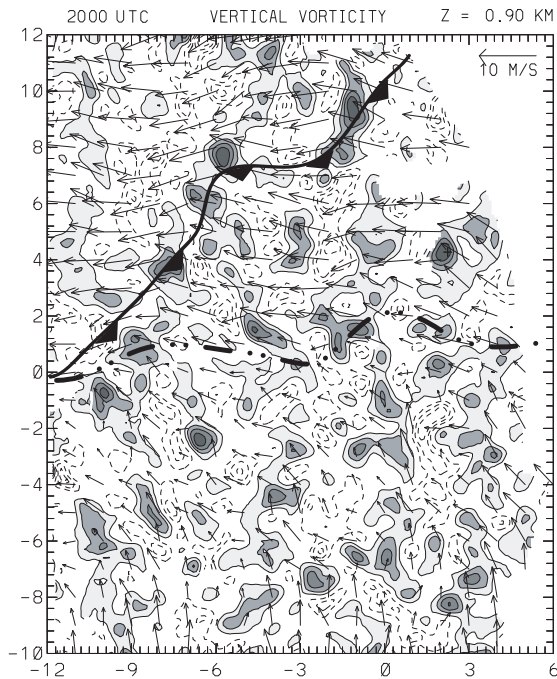


FIG. 5. Vertical vorticity, ζ , for 2000 UTC 12 June 2002 at an altitude of 900 m. Positive (negative) contours are solid (dashed) and contoured every $2.5 \times 10^{-3} \text{ s}^{-1}$ beginning at $1.5 \times 10^{-3} \text{ s}^{-1}$ ($-1.5 \times 10^{-3} \text{ s}^{-1}$). Areas exceeding $1.5 \times 10^{-3} \text{ s}^{-1}$ are shaded. Horizontal wind vectors are overlaid for every 10th grid point. The axes have units of km. The cold front is indicated using conventional symbology and an outflow boundary is indicated using the dash dotted line

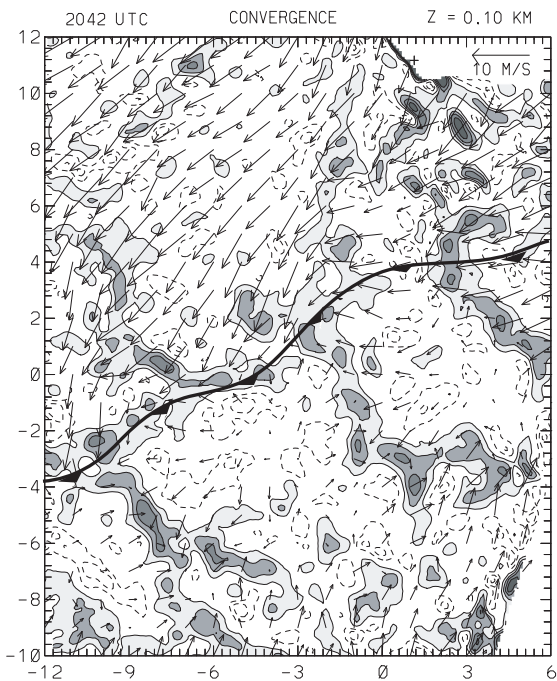


FIG. 6. Horizontal convergence, $-\nabla \cdot \mathbf{v}_h$, for 2042 UTC 12 June 2002 at an altitude of 100 m. Contours, winds, axes, and cold front are as in Fig. 3.

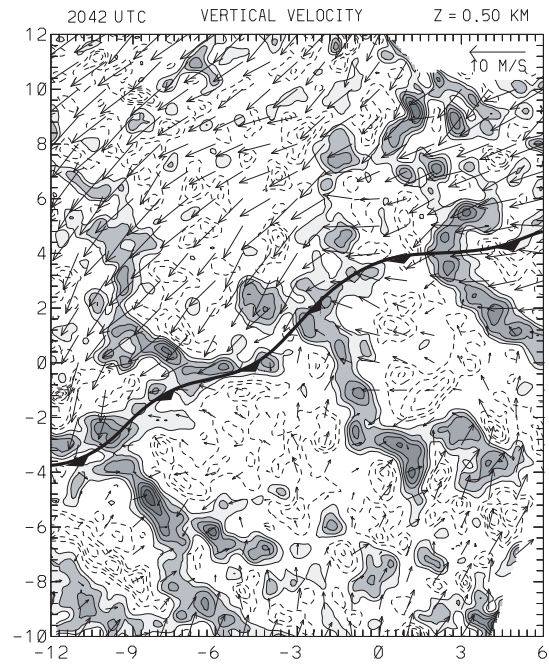


FIG. 7. Vertical velocity, w , for 2042 UTC 12 June 2002 at an altitude of 500 m. Contours, winds, axes, and cold front are as in Fig. 4.

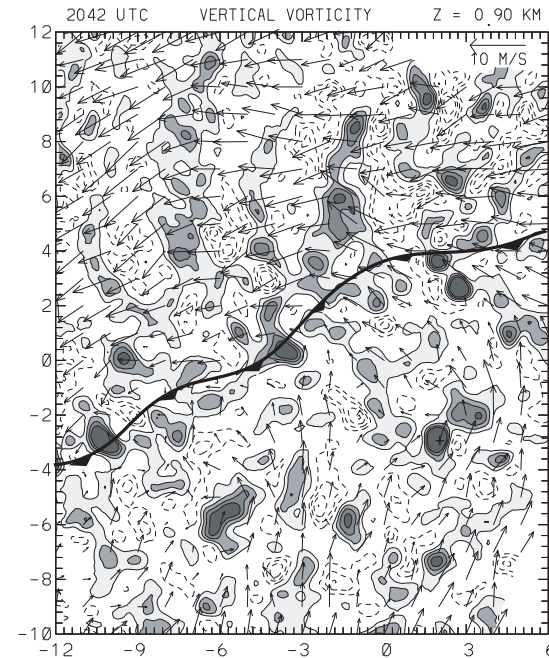


FIG. 8. Vertical vorticity, ζ for 2000 UTC 12 June 2002 at an altitude of 900 m. Contours, winds, axes, and cold front are as in Fig. 5.